Available online at www.sciencedirect.com
SCIENCE @ DIRECT®

Polymer 45 (2004) 2427–2432

polymer

www.elsevier.com/locate/polymer

Electrospun nylon 6 nanofiber reinforced BIS-GMA/TEGDMA dental restorative composite resins

Hao Fong[a,b,*]

[a]Department of Chemistry and Chemical Engineering, South Dakota School of Mines and Technology, Rapid City, SD 57701-3995, USA
[b]Anhui University of Technology and Science, Wuhu City, Anhui Province 241000, China

Received 2 December 2003; received in revised form 20 January 2004; accepted 22 January 2004

Abstract

Electrospun Nylon 6 nanofibers, in the form of nonwoven fabrics, were impregnated with the dental methacrylate of BIS-GMA/TEGDMA (50/50, mass ratio), to prepare the restorative composite resins. Three-point bending test results indicated flexural strength (FS), elastic modulus (E_Y) and work of fracture (WOF) of the nanofiber reinforced composite resins were all significantly increased with relatively small amounts of Nylon 6 nanofibers. The addition of 5% (mass fraction) nanofibers improved FS by 36%, E_Y by 26%, and WOF by 42% over those of the neat resin. SEM observations showed the fracture surface of the composite resin was rough, while the fracture surface of the neat resin was smooth and had large fracture steps. It is suggested that the presence of nanofibers deflected the crack. When the crack finally broke away from the nanofibers, numerous fracture lines and steps were created on the fracture surface, resulting in energy consumption during fracture.

Keywords: Dental restorative composites; BIS-GMA/TEGDMA; Electrospun nanofiber

1. Introduction

Developed over 40 years ago [1,2], polymeric dental restorative composites consist of methacrylate resin matrix and silanized glass or ceramic fillers. These materials presented opportunities never before equaled in modern dentistry, and have been widely accepted by the profession to replace traditional ‘dental amalgams’, alleviating both safety and cosmetic concerns.

The resin matrix is usually cured (hardened) by photo-initiated free radical polymerization. The monomer 2,2′-bis-[4-(methacryloxypropoxy)-phenyl]-propane (BIS-GMA) is one of the most commonly used base monomers. BIS-GMA is a very viscous, honey-like liquid. To improve the handling qualities, a low viscosity diluent monomer, such as tri (ethylene glycol) dimethacrylate (TEGDMA), is added to thin the resin [2]. In the BIS-GMA/TEGDMA system, BIS-GMA functions to limit polymerization shrinkage and enhance resin reactivity, while TEGDMA provides for increased methacrylate double bond conversions [3,4]. Besides resin matrix, dental restorative composite is also reinforced with inorganic fillers in the concentration up to about 70% (mass fraction). While the types of fillers are varied, most consist of short glass fibers, silica and ceramic particles or whiskers [5–7]. Based upon a number of laboratory studies, the mechanical properties of the composite materials were not substantially different from those of ‘dental amalgams’, so that composites can serve as a dental restorative materials [8]. However, investigations of the composite materials carried out over longer time periods were considerably less optimistic. Specifically, after 12–18 months of services, the degree of wear or loss of anatomical form was shown to be extensive [9–12].

Investigations into reasons for failure revealed that, among other reasons, the inorganic filler particle was a major contributor [13,14]. Ironically, the inorganic filler which had been added to the resin for the purpose of fortifying the material was actually responsible, at least in part, for its demise. During function, masticatory stresses were transmitted through the bolus of food and onto the surface of the particles projecting from the occlusal surface.

---

[*] Address: Department of Chemistry and Chemical Engineering, South Dakota School of Mines and Technology, Rapid City, SD 57701-3995, USA. Tel.: +1-605-394-1229; fax: +1-605-394-1232.
E-mail address: hao.fong@sdsmt.edu (H. Fong).

0032-3861/$ - see front matter © 2004 Elsevier Ltd. All rights reserved.
doi:10.1016/j.polymer.2004.01.067

Since the particles were considerably harder than the resin matrix in which they were embedded, much of the stress was transmitted through the particle and into the resin itself. Wherever the submerged portion of the particle was angulated or irregular in shape, the stress concentrations became excessively high. Such a condition tended to generate small cracks around the particle, thereby weakening the matrix locally.

Based on the above information, the investigation was carried out to examine the reinforcing effects of electrospun Nylon 6 nanofibers on the BIS-GMA/TEGDMA dental restorative resin matrix. The Nylon 6 nanofibers were much softer than inorganic fillers, and had a regular cylindrical shape. In the process of electrospinning [15–19], the key phenomenon of bending instability could result in the electrospinning jet being elongated up to 100,000 times in less than one tenth of a second [19]. This extremely large draw ratio could produce extended chain conformations and influence the formation and structure of polymer crystallites. Therefore, the electrospun polymer nanofibers could be very strong. Meanwhile, the small diameter of nanofibers also provided a high ratio of surface area to volume, which can enhance the intermolecular hydrogen bonding between the filler of Nylon 6 nanofibers and the matrix of BIS-GMA/TEGDMA resin, and thereby resulted in good interfacial properties of the composite resins. Since in the composite resins, the strength of filler and the interfacial properties of filler and matrix greatly impact the maximum strength, the Nylon 6 nanofiber reinforced composite resins are expected to be strong.

2. Experimental

2.1. Materials

Nylon 6 (catalog number 18,111-0), and the solvent 1,1,1,3,3,3-hexa-fluoro-2-propanol (HFIP) were purchased from Aldrich. BIS-GMA and TEGDMA monomers, as shown in Fig. 1, were supplied by Esstech (Essington, PA). The commonly used photo-initiator camphorquinone (CQ) and co-initiator ethyl-4 (*N*,*N*′-dimethylamino) benzoate (4EDMAB), as shown in Fig. 1, were selected as the photo-initiation system. CQ and 4EDMAB were also purchased from Aldrich Chemical Co. All materials were used as received without further purification.

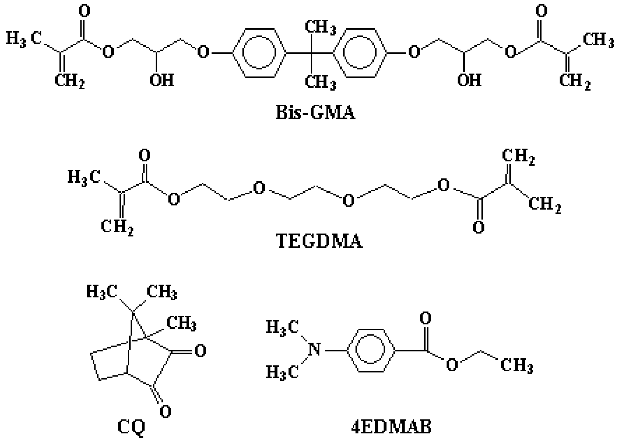

Fig. 1. Molecular structures of dental monomers and initiators.

2.2. Electrospinning

The electrospinning apparatus used a high voltage power supply (ES30P, 200 μA at 30 kV), purchased from Gamma High Voltage Research (Ormond Beach, FL). During electrospinning, a positive high voltage was applied through a copper wire to a solution of 10% (mass fraction) Nylon 6 dissolved in HFIP. The solution was placed inside a common glass pipette, and the capillary tip diameter of the pipette was about 1.2 mm. A grounded metal sheet was placed 25 cm below the tip of the glass pipette. The pipette was tilted a few degrees from the horizontal so that surface tension maintained a small droplet of the solution at the tip. As the electrical potential was gradually increased to 20 kV, a jet was created. The jet, formed by electrical forces, followed a complicated stretching and looping path as it dried and solidified. Nonwoven fabric was formed on the surface of a piece of aluminum foil, which covered the grounded metal sheet. The fabric could easily be peeled off the aluminum foil after immersion in ethanol (or distilled water). The Nylon 6 nanofibers had very high aspect ratio (i.e. no fiber end was identified during SEM observations). The collected nonwoven fabric was about 15 cm wide and 20 cm long, with a compressed thickness of about 30 μm. The mass per unit area of the fabric was about 75 g/m^2.

2.3. Sample preparation and evaluation

The peeled electrospun fabric was placed in a 100 °C vacuum oven (~27.9 kPa) overnight to completely remove the solvent and allow the Nylon 6 to anneal. Then pieces, 25 mm long and 2 mm wide, were carefully cut from the fabric, to fit the mold of a 3 point bending specimen. These pieces were subsequently immersed into the activated dental monomer mixture of BIS-GMA/TEGDMA (50/50 mass fraction, activated with the photo initiator CQ (mass fraction of 0.2%) and the co-initiator 4EDMAB (mass fraction of 0.8%). Ultrasonic vibration was employed to remove the trapped air bubbles in the immersed pieces. After overnight immersion, the fabric pieces were swollen completely without any visible air bubbles. Specimens for 3 point bending test were made using layers of completely soaked nanofiber fabric pieces and an extra amount of activated BIS-GMA/TEGDMA monomers, as shown schematically in Fig. 2. In the preparation of the 3 point bending specimen, one layer of fabric contributed approximately 2.5% (mass fraction) of Nylon 6 in the composite resin. The 3 point bending samples were photo-cured for 2 min using 'TRIAD

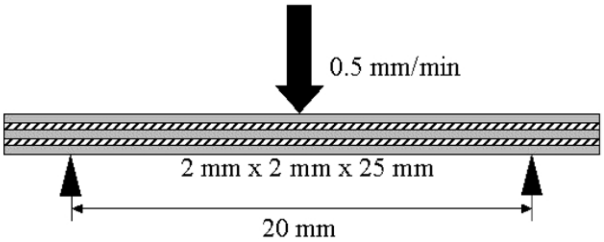

Fig. 2. Schematic drawing of 3 point bending test used in this study. The two thin striped bars (could also be one or three) inside the specimen represent BIS-GMA/TEGDMA impregnated electrospun Nylon 6 fabrics, and the shadowed areas represent BIS-GMA/TEGDMA resin without nanofibers.

2000' photo curing chamber, purchased from Dentsply International, Inc. (York, PA). All the above sample preparations were conducted in a yellow-light room to avoid the premature curing.

2.3.1. Flexural strength, elastic modulus and work of fracture

Flexural strength (FS), elastic modulus (E_Y) and work of fracture (WOF) of the composite resins were tested using a standard 3 point bending test method (ASTM F417-78, 1984). Prior to mechanical testing, the specimens were immersed in distilled water at 37 °C for 24 h, followed by the careful polish on all four sides with 2400 grit silicon carbide paper and water coolant in a longitudinal direction. The final dimensions of the specimens were then measured and recorded. The specimens were fractured in a three point bending jig with a 20 mm span on a computer-controlled Universal Testing Machine (model 5500R, Instron Corp., Canton, MA) at a cross-head speed of 0.5 mm/min to record stress strain curves. Calculations were made using the following formulas:

$$\mathrm{FS} = 3PL/2WT^2$$

$$E_y = (P/d)(L^3/4WT^3)$$

$$\mathrm{WOF} = A/(WT)$$

Where P is the load at fracture, L is the distance between two supports (which was set to be 20 mm), W is the width of the specimen, T is the thickness of the specimen, and d is the deflection, in millimeters, at load P. In the formula of WOF, A is the area under the load-displacement curve, which is the work done by the applied load to deflect and fracture the specimen. With the unit of A being J (Joules), the unit of WOF (or fracture resistance) is J/m^2 or more conveniently, kJ/m^2 [20,21]. Eight specimens, approximately 25 mm in length, 2 mm in width and thickness were prepared and tested.

2.3.2. Scanning electron microscope

Selected fracture surfaces of the 3 point bending specimens were examined by a Scanning Electron Microscope (SEM, model JSM-5300, JEOL, Peabody, MA) to investigate fracture origins (e.g. air bubbles, nanofiber agglomerates) and crack-filler interactions (e.g. fracture of nanofiber, nanofiber pullout). Prior to SEM observations, the samples were sputter coated with a thin layer (~5 nm) of gold to allow for better electrical conduction.

3. Results and discussion

The electrospun Nylon 6 nanofibers made in this study had diameters ranging from 100 to 600 nm. When observing these nanofibers with a backscattered polarized light, different interference colors were seen from fibers of different diameters. Birefringence characteristic of nanofibers was observed by rotating the fibers between crossed polarizers in an optical microscope, which implied the macromolecules extended along the fiber axis.

Fig. 3(a) is a SEM image showing the representative morphology of the electrospun Nylon 6 nanofibers. Although the fibers were quite uniform, the diameter deviation of several hundred nanometers was still observed.

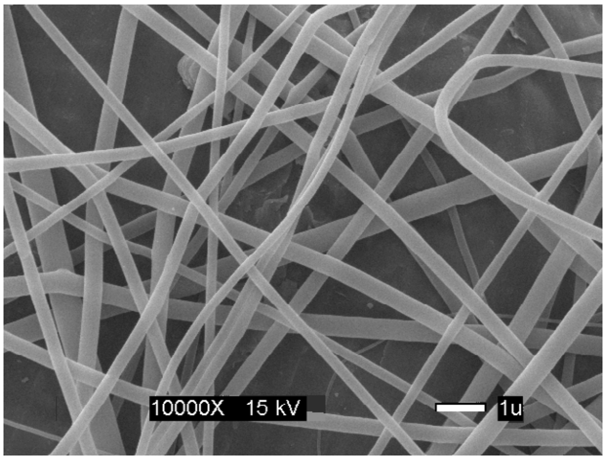

(a)

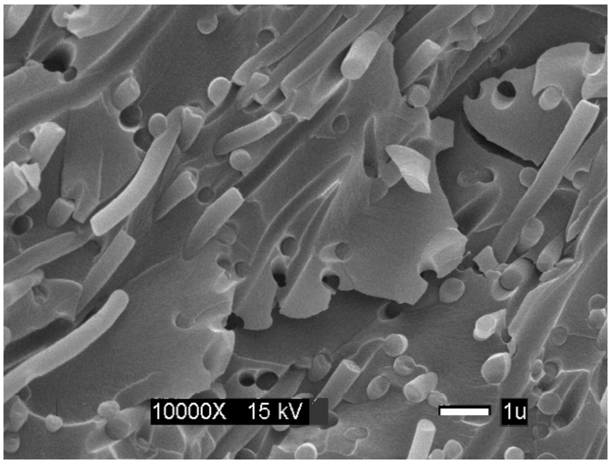

(b)

Fig. 3. Scanning electron micrographs of (a) electrospun Nylon 6 nanofibers in the form of nonwoven fabric, (b) representative fracture surface showing the presence of the nanofibers in the composite resin.

However, the nanofibers were very smooth, and no beaded nanofibers [16] were seen within the scope of this SEM observation. It should be addressed that the fabric as shown in Fig. 2(a) was purposely collected for SEM observation, and the actual fabric used for fabrication of the composite resins was much denser.

After the fabric pieces were immersed and completely soaked with the mixture of activated BIS-GMA/TEGDMA monomers, the thickness of the fabric expanded many times thicker. This process converted the Nylon 6 nanofibers from the dense nonwoven fabric to the scaffold-like, highly interpenetrated, highly porous framework. After the photo-polymerization, although the overall structure of the composite resin was a laminate, yet within the layer containing the nanofiber fabric, the structure was similar to the interpenetration network. SEM images of the representative presence of the nanofiber in the composite resins were shown in Fig. 3(b). The nanofibers were randomly distributed with no clear alignment. The bonding between nanofibers and BIS-GMA/TEGDMA matrix was reasonably good, since embedded nanofibers tended to break instead of pullout during the 3 point bending test. Furthermore, the nanofibers were closely surrounded by the matrix resin, showing that the matrix resin had remained in intimate contact with the nanofibers' surfaces and had not shrunk away. Nevertheless, if the nanofiber incidentally aligned along the breaking direction, peel-off could also happen (Fig. 3(b)). Within the scope of this SEM observation, the presence of resin remnants on the ends of the pullout fibers was rarely found. This might indicate that the interface between the filler and the matrix still needed to be further improved. Meanwhile, numerous small holes were presented in Fig. 3(b). Although these holes had various depths, but overall, they are quite shallow. These holes were the result of breaking the fibers. If the fiber broke not exactly on the fracture surface, but close to the surface, and the broken end was then pulled out, these shallow holes would be created. The presence of these holes implied that the fibers absorbed stress during the breaking, and resulted in a reinforcement of the composite resin.

The comparison of the fracture surfaces between the nanofiber reinforced composite resin and the neat resin was shown in Fig. 4(a) and (b), respectively. The direction of the crack propagation during the 3-point bending test was approximately from top to bottom in each micrograph. The fracture surface of the nanofiber reinforced composite resin (Fig. 4(a)) was very rough, while the fracture surface of the neat resin (Fig. 4(b)) was much smoother. Meanwhile, the neat resin sample had relatively large fracture steps, indicating little resistance to the applied force, and implying the nanofibers could deflect the crack. When the crack finally broke away from the nanofibers, numerous fracture lines and steps were created in the fracture surface, suggesting energy consumption during breaking.

The mechanical properties of the Nylon 6 nanofiber reinforced composite resins with 1, 2 or 3 layers of Nylon 6 nanofiber fabrics, as well as the control samples of neat BIS-GMA/TEGDMA (50/50, mass ratio) resins, were measured and shown in Fig. 5. Each layer of fabric contributed 2.5% (mass fraction) of Nylon 6 nanofibers in the composite resin. Thus, 1, 2 and 3 layers of fabrics represented the mass fractions of 2.5, 5.0 and 7.5% of nanofibers in the composite resins, respectively. Each bar in the plots of Fig. 5 represented the mean value of eight measurements, with the error bar showing one standard deviation.

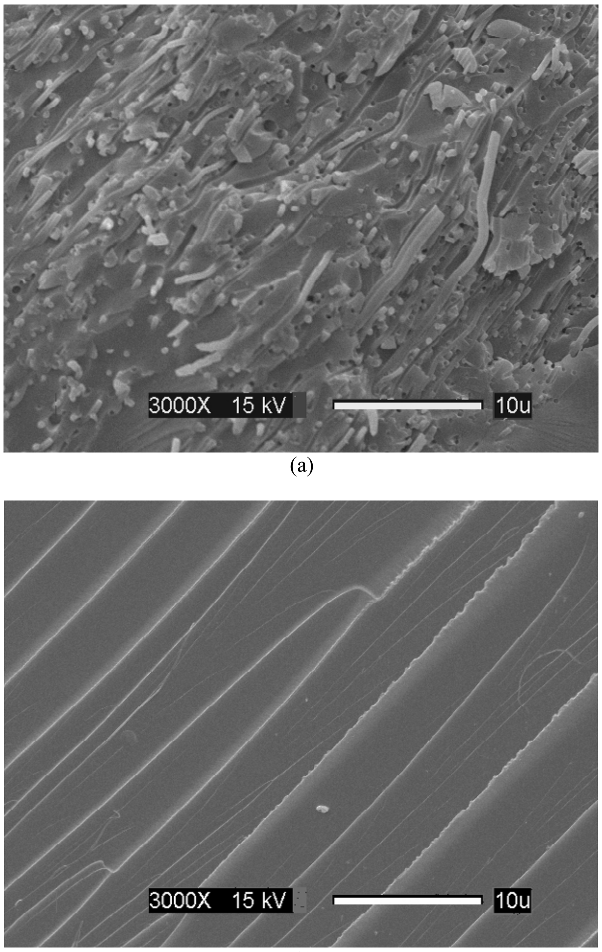

Fig. 4. Scanning electron micrographs of fracture surfaces of representative 3 point bending specimen: (a) composite resin with 2 layers of nanofiber fabrics (image taken at the place where the nanofibers were presented), (b) neat resin without nanofibers.

With embedding relatively small amounts of Nylon 6 nanofibers in the dental resin matrix, FS, elastic modulus (E_Y) and WOF of the composites were all distinguishably increased. FS, E_Y and WOF of the neat resin (mean ± standard deviation, $n = 8$) were (79.8 ± 3.1) MPa, (2064 ± 73) MPa and (5.66 ± 0.85) kJ/m^2, respectively. For the 2.5% (mass fraction) nanofiber filled composite, FS, E_Y and WOF were increased to (94.6 ± 9.5) MPa, (2319 ± 106) MPa and (6.87 ± 0.98) kJ/m^2, respectively. When the mass fraction of Nylon 6 increased to 5.0% (mass fraction), the FS, E_Y and WOF were (108.8 ± 11.8) MPa,

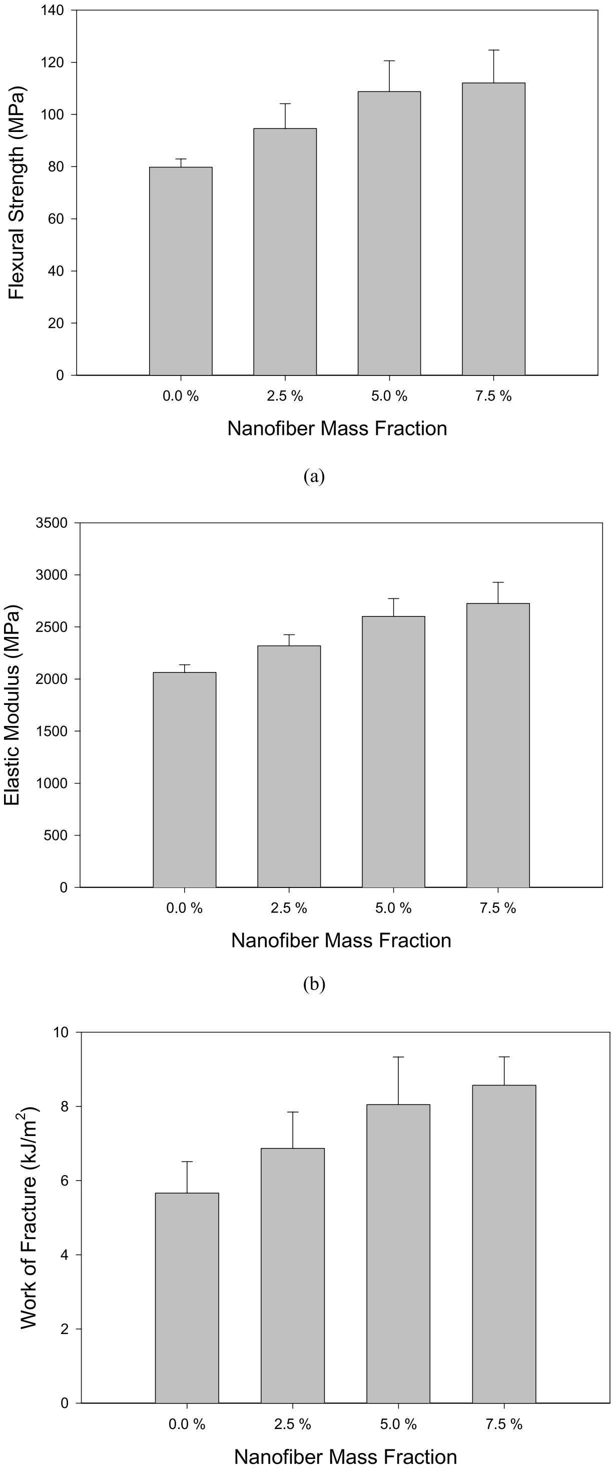

(a)

(b)

(c)

Fig. 5. Mechanical properties: (a) flexural strength, (b) elastic modulus and (c) work of fracture, of the composite resins containing different amounts (layers) of Nylon 6 nanofiber nonwoven fabrics. Each datum is mean with error bar showing one standard deviation (SD), $n = 8$.

(2601 ± 170) MPa and (8.05 ± 1.28) kJ/m^2, which almost doubled the improvement in comparison with the 2.5% filled samples. From the neat resin to the 5.0% nanofiber filled composite resin, the FS was improved by 36%, elastic modulus was improved by 26%, and the WOF was improved by 42%. However, continuously increasing the nanofiber's mass fraction to 7.5% did not further improve the mechanical properties of the composite resins significantly. As shown in Fig. 5, for the 7.5% nanofiber filled composite resins, FS, E_Y and WOF (mean ± standard deviation, $n = 8$) were (112.1 ± 12.6) MPa, (2726 ± 203) MPa and (8.57 ± 0.77) kJ/m^2, which were statistically the same as the samples with 5.0% filler level (one way analysis of variance (ANOVA), $P > 0.05$). The reasons for this are still under investigation. Arguably, there were two reasons: (1) since the nanofiber nonwoven fabrics were laminated into the matrix layer by layer, and the interpenetration of fibers between the layers was less likely, the addition of extra layer of fabric did not significantly increase the nanofiber density locally at the breaking point; (2) the improvements of mechanical properties of the composites might be limited by the interface between the nanofiber and the matrix. As discussed earlier, almost no resin remnants could be identified on the ends of the pullout fibers, which implied additional surface treatments might be needed to further improve the mechanical properties of the composite resins.

It is also noticed that, through embedding of Nylon 6 nanofibers, both the FS and the WOF of the composite resins could be improved simultaneously. Suggested reasons are that, the nanofibers which were strongly bonded to the methacrylate matrix caused the improvement of the strength, while the nanofibers which were pulled out from the matrix created the frictional force, and the frictional force allowed stress transfer across matrix cracks, and therefore increasing the material resistance to fracture. Thus, the strength of the composite resins could be potentially tailored with the toughness by controlling the nanofiber/matrix interfacial strength.

Finally, although in this study electrospun Nylon 6 nanofibers were embedded in the BIS-GMA/TEGDMA resins as the form of nonwoven fabric stripes, the actual dental application might require the fabric to be cut into much smaller pieces in order to mix well with the dental monomers, and to make the applicable dental paste. Nevertheless, since relatively small amounts (e.g. 5.0% mass fraction) of nanofibers could effectively increase the overall mechanical properties of the dental restorative composite resins, the nanofibers might have a bright future to be used as the reinforcing filler in the dental restorative composites.

4. Summary

The objective of this research was to study the reinforcing effects of Nylon 6 nanofibers on the BIS-GMA/TEGDMA dental restorative composite resin matrix. Nylon 6 nanofibers was electrospun using the 10% (mass fraction) HFIP solution, and collected as the nonwoven fabric. The nanofibers had a uniform cylindrical shape, with the diameter less than 1 μm, which is about one tenth the diameter of the ordinary textile fibers. The nanofibers showed strong birefringence when observed under polarized optical microscope, which suggested oriented Nylon 6 crystalline structure, and implied that the Nylon 6 nanofibers were mechanically strong. The small diameter of nanofibers also provided a high ratio of surface area to volume, which could enhance the intermolecular hydrogen bonding between the filler of Nylon 6 nanofiber and the matrix of BIS-GMA/TEGDMA resin, and further resulted in good interfacial properties of the composite resins.

The mechanical properties of the nanofiber reinforced composite resins were tested using standard 3 point bending test method. The specimens were prepared using layers of completely pre-soaked nanofiber fabric pieces and extra amount of activated BIS-GMA/TEGDMA monomers. Photo polymerization was applied to cure the specimens. The results of 3 point bending tests indicated that FS; elastic modulus (E_Y) and WOF of the composite resins could all be significantly increased after impregnating relatively small amount of Nylon 6 nanofibers. The addition of 5% (mass fraction) nanofiber in the resin could improve FS by 36%, E_Y by 26%, and WOF by 42%. SEM observations showed that the fracture surface of the fiber-reinforced composite resin was very rough, and the fracture surface of the neat resin sample was relatively smoother with much larger fracture steps. This suggested that the presence of nanofibers could effectively deflect the crack. When the crack finally broke away from the nanofibers, numerous fracture lines and steps were created on the fracture surface, suggesting energy consumption during breaking. If the nanofibers coincidentally aligned along the breaking direction in the composite resins, peel-off could also happen. Nevertheless, there is little SEM evidence to show the presence of resin remnants on the end of the pullout fibers. These might imply that the interface between the filler of Nylon 6 nanofibers and the matrix of BIS-GMA/TEGDMA resin still needs improvement to further fortify the dental restorative composite resins.

Acknowledgements

This work was supported by the National Science Foundation/EPSCoR Grant#EPS-0091948 and by the State of South Dakota, and also by the American Dental Association Foundation. The author is grateful to Esstech for the generous donation of the BIS-GMA and TEGDMA monomers used in this study. The author would also like to acknowledge the helpful discussions with Dr Sabine H. Dickens, Dr Joseph M. Antonucci and Dr Hockin H.K. Xu, at the National Institute of Standards and Technology and at the Paffenbarger Research Center of the American Dental Association.

References

[1] Bowen RL. US Patent No. 3, 066, 112; 1962.
[2] Mabie CP, Menis DL. J Biomed Mater Res 1978;12:435.
[3] Reed BB, Choi K, Dickens SH, Stansbury JW. Polym Preprint 1997; 38(2):108.
[4] Antonucci JM, Stansbury JW. Molecular designed dental polymer. In: Arshady R, editor. Desk reference of functional polymers: synthesis and application. American Chemical Society Publication; 1997.
[5] Jordan RE, Suzuki M. J Am Dent Assoc 1991;122:31.
[6] Ferracane JL, Mitchem JC. Dent Mater 1994;10:92.
[7] Xu HK, Martin TA, Antonucci JM, Eichmiller FC. J Dent Res 1999; 78(2):706.
[8] Phillips RW, Avery DR, Mehra R, Swartz ML, McCune RJ. J Prosthet Dent 1971;26:68.
[9] Phillips RW, Avery DR, Mehra R, Swartz ML, McCune RJ. J Prosthet Dent 1972;28:164.
[10] Phillips RW, Avery DR, Mehra R, Swartz ML, McCune RJ. J Prosthet Dent 1973;30:891.
[11] Leinfelder KF, Sluder TB, Sockweli CI, Strickland WD, Wall JT. J Prosthet Dent 1975;33:407.
[12] Leinfelder KF, Sluder TB, Santos JFE, Wall JT. Oper Dent 1980;5:57.
[13] Kusy RP, Leinfelder KF. J Dent Res 1977;56:544.
[14] Abell AK, Leinfelder KF, Turner DT. J Biomed Mater Res 1983;17: 501.
[15] Reneker DH, Chun I. Nanotechnology 1996;7:215.
[16] Fong H, Chun I, Reneker DH. Polymer 1999;40:4585.
[17] Fong H, Reneker DH. J Polym Sci B 1999;37:3488.
[18] Fong H, Reneker DH. In: Salem DR, Sussman MV, editors. Structure formation in polymeric fibers: Chapter 6, electrospinning and formation of nanofibers. Hanser; 2001.
[19] Reneker DH, Yarin AL, Fong H, Koombhongse S. J Appl Phys 2000; 87:4531.
[20] Xu HHK, Ostertag CP, Fuller ER, Braun LM, Lloyd IK. J Am Ceram Soc 1995;78:698.
[21] Xu HHK, Eichmiller FC, Giuseppetti AA. J Biomed Mater Res 2000; 52:107.